Supplement of Atmos. Chem. Phys., 23, 3575–3593, 2023
https://doi.org/10.5194/acp-23-3575-2023-supplement

Atmospheric Chemistry and Physics
Open Access
EGU

Supplement of

Local and remote climate impacts of future African aerosol emissions

Christopher D. Wells et al.

Correspondence to: Christopher D. Wells (c.d.wells@leeds.ac.uk)

In addition to the coupled ocean-atmosphere idealised experiments, a 26-year simulation with fixed SSTs and sea ice was performed for each experiment to determine the ERF imposed by each instantaneous emissions perturbation. The 10×Trop-OCBC experiment resulted in an ERF of 1.6 ± 0.1 W m^{-2}. This positive forcing indicates that the absorbing black carbon aerosol outweighs the effect of the scattering organic carbon, and reflects a balancing of a positive atmospheric forcing of 5.6 ± 0.1 W m^{-2} and a negative surface forcing of -4.0 ± 0.1 W m^{-2}. In contrast to this large atmospheric forcing via BC, the negative ERF of -3.0 ± 0.1 W m^{-2} under the 10×Trop-SO_2 experiment reflects a small positive atmospheric forcing of 0.16 ± 0.08 W m^{-2}, likely due to increased BC absorption via enhanced SW reflection. The surface forcing is then similar to the ERF, at -3.2 ± 0.1 W m^{-2}.

The subsequent figures show results from the couped ocean-atmosphere idealised experiments.

Figure S1 shows the surface temperature response in DJF and JJA to each idealised aerosol emissions perturbation, as Figure 4 showed for the scenario experiments. Consistent with the dominance of carbonaceous aerosol within the scenario experiments, and BC within that, the increased BB OC+BC experiments show strong warming, with local cooling tracking the BB seasonal cycle. Reduced BB OC+BC emissions, consistently and in contrast, generate a general cooling and local warming. Increased SO_2 emissions drive a strong cooling, as expected given their scattering properties, which are strong in UKESM1 (Thornhill et al., 2021). An anomalous warming feature is present in the southern ocean south of the Pacific, particularly in JJA; this appears to be large-amplitude internal variability in one member, and even appears in the global mean temperatures in Figure 2 for one member of 10×Trop-SO_2, late in the simulation. Arctic amplification of the general temperature response is clear in DJF in each experiment.

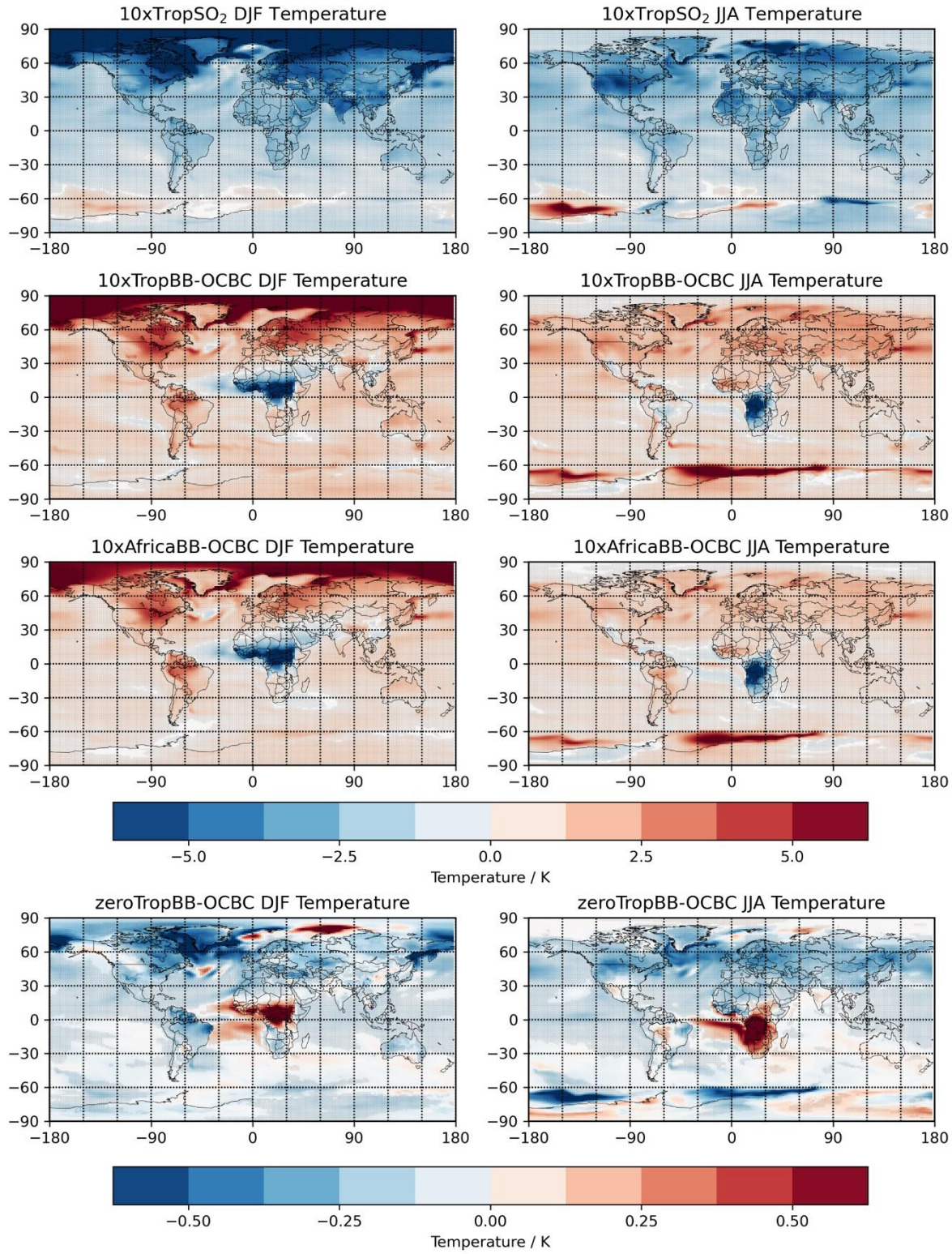

Figure S1: Effect of each idealised perturbation experiment on surface temperatures in DJF (left) and JJA (right) in years 50-200 of the perturbation (the 1st 50 years are discarded a spin-up). Stippling indicates gridcells where the change is significant with respect to intra-ensemble variation.

Figure S2 shows the changes in vertical velocity at 850hPa and zonally across the Atlantic, in DJF and JJA, in the idealised experiments. Increased SO_2, primarily in the northern hemisphere, drives a

southward ITCZ shift in both seasons across each basin. The Pacific sees a northward DJF shift under increased carbonaceous aerosol, consistent with the northern hemisphere positive forcing in this season. A converse southward shift occurs under 10×TropBB-OCBC in JJA, as the positive forcing is centred in the southern hemisphere in this season. However, this Pacific shift is not realised in 10×AfricaBB-OCBC; a seemingly northward shift again appears, though this doesn't persist to higher altitudes (not shown). Over the Atlantic, consistent shifts seem to appear under the increased carbonaceous aerosol experiments, but these do not line up with the ITCZ itself, and indicate a local circulation response to the large emissions changes. Instead, the smaller zeroTropBB-OCBC experiment shows coherent ITCZ shifts in the Atlantic in JJA and DJF, indicating that larger perturbations don't simply result in clearer features of the response.

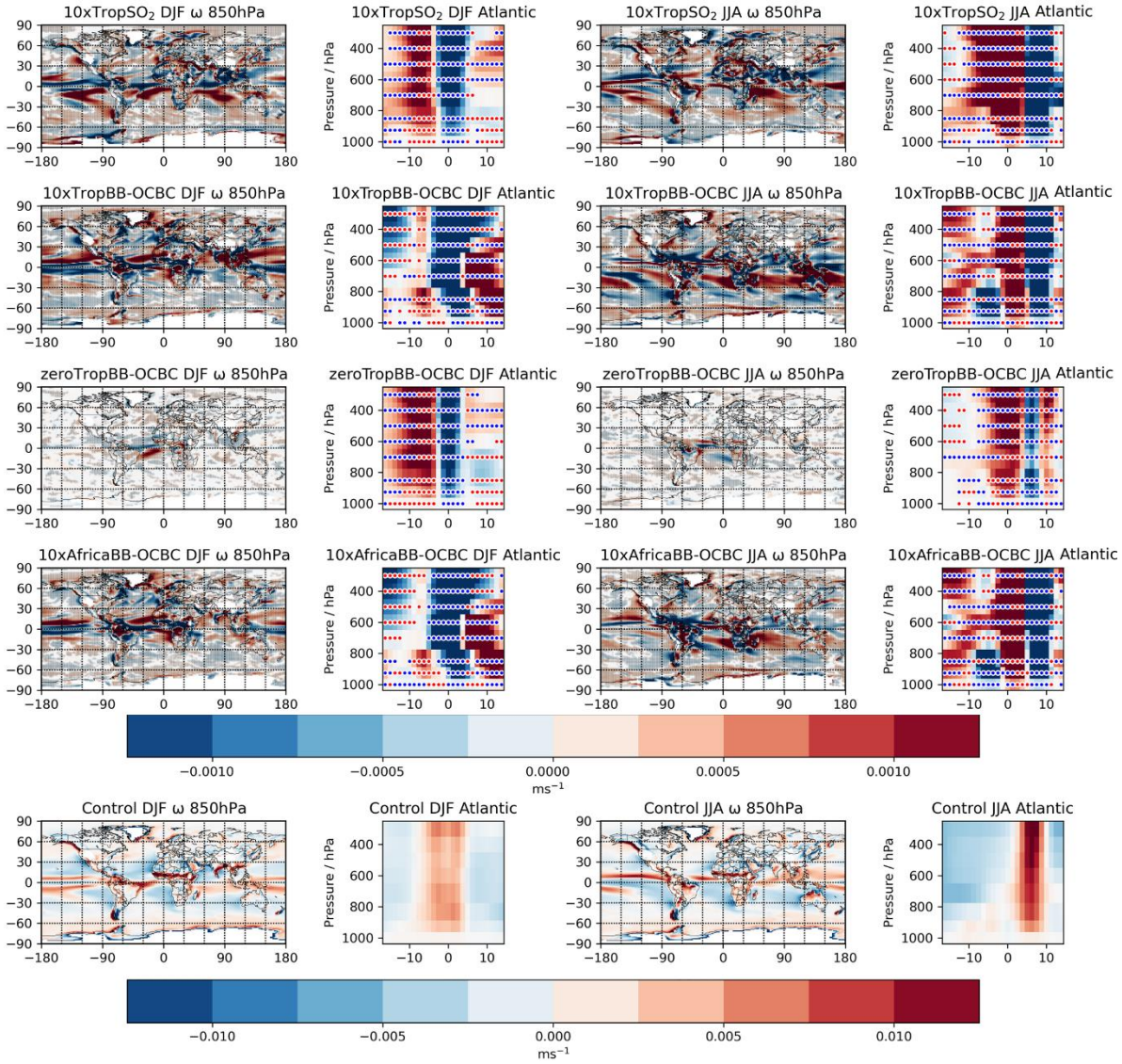

Figure S2: Vertical velocity changes globally, and zonally over the Atlantic (40W − 15W) in DJF and JJA, for the idealised experiments, for years 50-200 after the perturbation. Stippling on the change plots indicates gridcells where the change is significant with respect to the intra-ensemble variation. The stippling on the zonal plots is coloured red when the change strengthens the background circulation, and blue when opposing.

Figure S3 presents the precipitation change in DJF and JJA under the idealised experiments, with global and Pacific means indicated too. Increasing SO_2 aerosol drives large general decreases via atmospheric cooling, with strong southwards ITCZ shifts as in the vertical velocity response. Conversely, the warming under increased carbonaceous aerosol drives remote increases, though global precipitation is decreased here due to the increased atmospheric absorption under increased BC aerosol. The effects of ITCZ shifts are again seen, most clearly in the Pacific, with zeroTropBB-OCBC showing primarily local features consistent with those under AerBB.

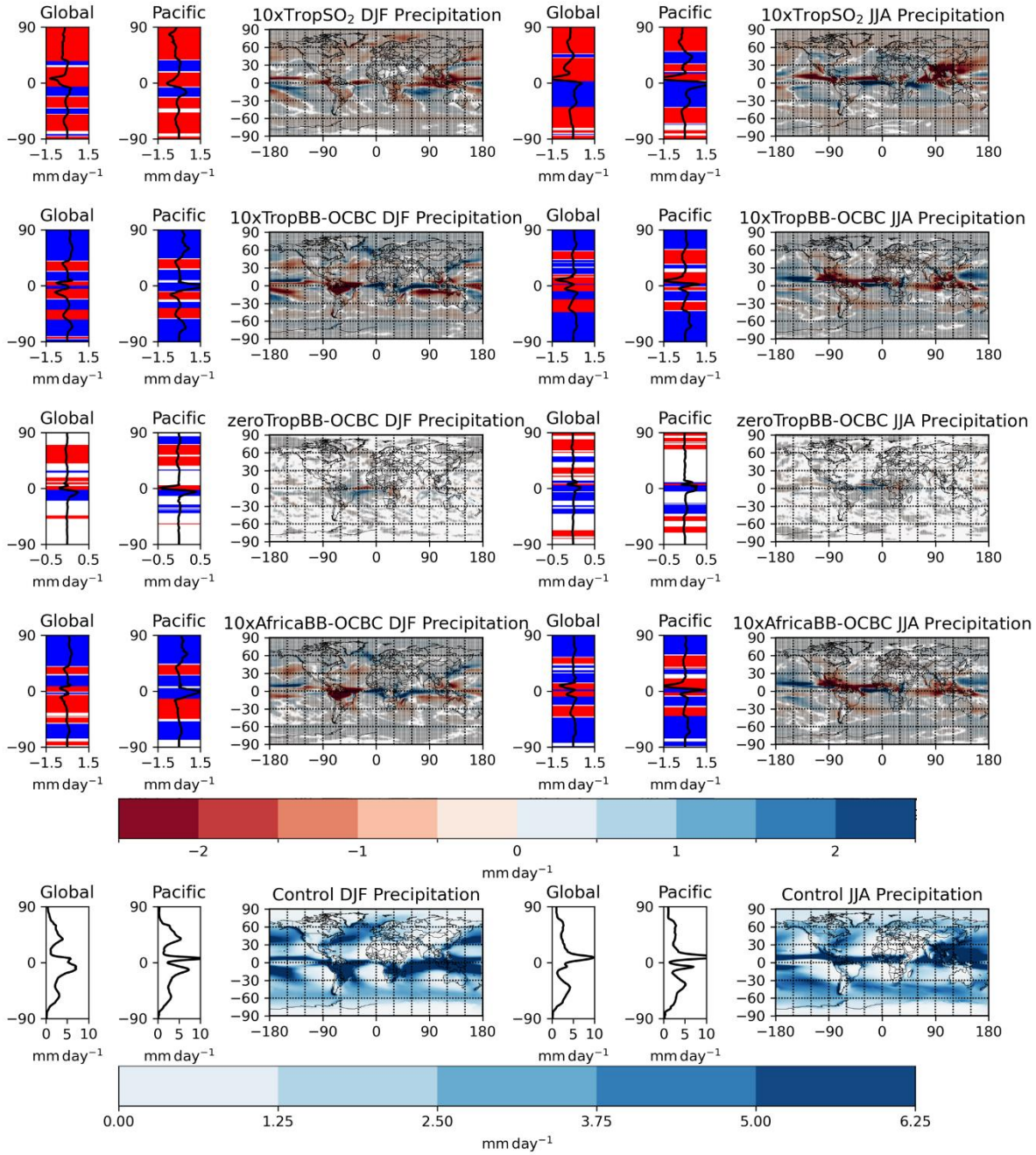

Figure S3: Precipitation response in years 50-200 of the idealised experiments relative to the control for DJF (left) and JJA (right), with maps and zonally both globally and across the Pacific (150E − 270E). Control DJF and JJA precipitation maps are shown at the bottom. Stippling on the maps indicates

gridcells where the change is significant with respect to intra-ensemble variation. The coloured areas in the zonal change plots show significance – red for decreased, blue for increased precipitation.

The line profile analysis, presented in Figure 8 of the main text for several region-season pairs in the scenario experiments, is shown in Figure S4 for the idealised experiments in DJF, over East Africa (defined in Figure 9 of the main text). This is a region with strongly increased emissions and background convection (Figure S2), and therefore demonstrates the precipitation-enhancing mechanism discussed in the main text. Increased carbonaceous aerosol emissions generate strong burden increases throughout the column, with the characteristic vertical temperature response, including the warming peak, and the enhanced circulation and precipitation as a result (Figure S3). Conversely, reduced BB aerosol emissions trigger the exact opposite response: a mid-tropospheric stability anomaly caused by a local cooling peak, leading to suppressed local precipitation.

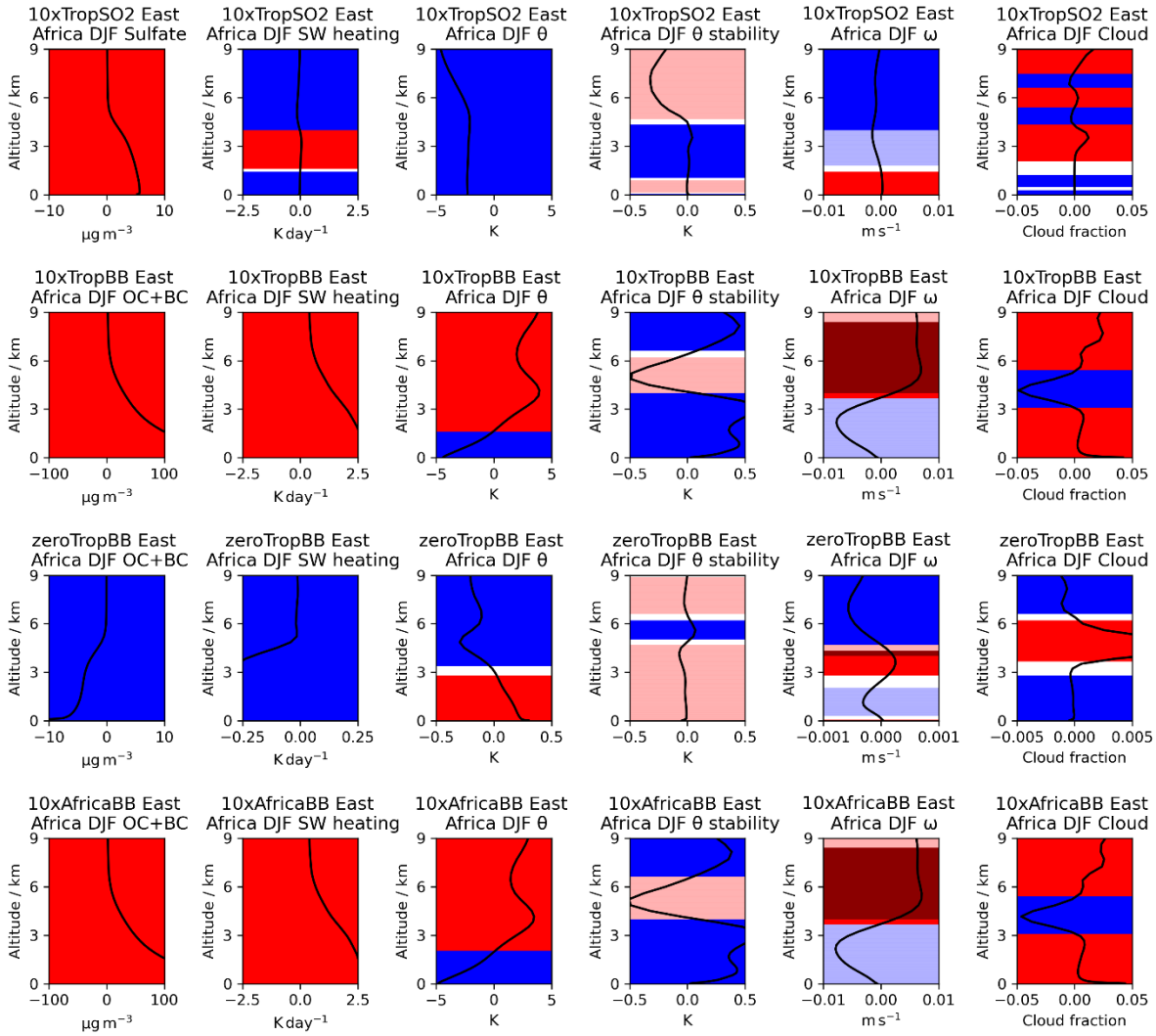

Figure S4: Changes in the vertical profile of perturbed aerosol burden (left column), clear-sky SW heating (2nd column), potential temperature (3rd column), potential temperature vertical gradient calculated at each level as the potential temperature at the height immediately above the level minus at that level (4th column), vertical velocity (5th column), and cloud (6th column), over East Africa (see Figure 9 in the main text), averaged over 50-200 years after the application of the

idealised perturbations relative to the control. Coloured horizontal lines indicate significant increases (red) or decreases (blue). The stability and vertical velocity colour shades are modified depending on the sign of the change relative to the control baseline: lighter red and blue when the change is enhancing the background, normal when opposite in direction to the background but with the change weaker in magnitude, and darker when opposed with higher magnitude than the control, acting to reverse the sign. Note the smaller scale, by a factor of 10, in zeroTropBB-OCBC's plots compared to the increased OC+BC experiments, and the smaller scale in the 10×Trop-SO_2 sulfate burden response.